J. Fluid Mech. (1972), *vol.* 55, *part* 1, *pp.* 1–23
Printed in Great Britain

A model for the micro-structure in ciliated organisms

By JOHN BLAKE

Department of Applied Mathematics and Theoretical Physics,
University of Cambridge

(Received 17 December 1971)

Improved models for the movement of fluid by cilia are presented. A theory which models the cilia of an organism by an array of flexible long slender bodies distributed over and attached at one end to a plane surface is developed. The slender bodies are constrained to move in similar patterns to the cilia of the micro-organisms *Opalina*, *Paramecium* and *Pleurobrachia*.

The velocity field is represented by a distribution of force singularities (Stokes flow) along the centre-line of each slender body. Contributions to the velocity field from all the cilia distributed over the plane are summed, to give a streaming effect which in turn implies propulsion of the organism. From this we have been able to model the mean velocity field through the cilia sublayer for the three organisms. We find that, in a frame of reference situated in the organism, the velocity near the surface of the organism is very small – up to one half the length of the cilium – but it increases rapidly to near the velocity of propulsion from then on. This is because of the beating pattern of the cilia; they beat in a near rigid-body rotation during the effective ('power') stroke, but during the recovery stroke move close to the wall. Backflow ('reflux') is found to occur in the organisms exhibiting antiplectic metachronism (i.e. *Paramecium* and *Pleurobrachia*). The occurrence of gradient reversal, but not backflow, has recently been confirmed experimentally (Sleigh & Aiello 1971).

Other important physical values that are obtained from this analysis are the force, bending moment about the base of a cilium and the rate of working. It is found, for antiplectic metachronism, that the force exerted by a cilium in the direction of propulsion is large and positive during the effective stroke whereas it is small and negative during the recovery stroke. However, the duration of the recovery stroke is longer than the effective stroke so the force exerted over one cycle of a ciliary beat is very small. The bending moment follows a similar pattern to the component of force in the direction of propulsion, being larger in the effective stroke for antiplectic metachronism. In symplectic metachronism (i.e. *Opalina*) the force and bending moment are largest in magnitude when the bending wave is propagated along the cilium. The rate of working indicates that more energy is consumed in the effective stroke for *Paramecium* and *Pleurobrachia* than in the recovery stroke, whereas in *Opalina* it is found to be large during the propagation of the bending wave.

1. Introduction

The topic of this paper is one of the many interesting subjects in the new and rapidly developing field of biomechanics, where a knowledge of both fluid mechanics and physiology is required. Cilia have many functions, existing in nearly all phyla of the animal kingdom and some of the plant kingdom. Some of the functions of cilia are in locomotion of micro-organisms, cleansing of gills, feeding, excretion and in reproduction. The mechanics of ciliary motion has interested both zoologists and fluid mechanists for many years. Both Gray (1928) and Prandtl (1952, p. 238) expressed considerable interest in the fluid mechanics of the cilium's movement. This present paper is directed towards the theory of the propulsion of micro-organisms by cilia, although it may have some applications to flow in large diameter tubes due to ciliary activity (e.g. mucus in the trachea). In micro-organisms we have the opportunity to observe cilia in their near natural surroundings which means that we can compare our theoretical models with the observations of the proto-zoologists. Many of the ideas of this paper have been gleaned from films on both cilia and flagella (Holwill & Sleigh 1967*a*; Winet 1970).

Micro-organism locomotion can be broadly split into two types, if we neglect the inefficient and ineffective movements due to jet propulsion and the peculiar movements of the amoeba. The first is the flagella type of propulsion, characterized by spermatozoa, which consists of a single (or several) long slender organelle, that exhibits a 'symmetrical' bending wave. The other type is that due to a dense covering of beating cilia over the external surface of micro-organisms. Cilia have the same internal structure as flagella but, however, tend to have highly asymmetrical beating patterns. Many cilia exhibit a three-dimensional motion as they beat as in fact do flagella when they beat in a helical movement (see, for example, Chwang & Wu 1971).

The classical cilium beat can be split into two parts, one being the effective ('power') stroke, in which the cilium (or 'combplate') beats in a near rigid-body rotation about the base, while during the recovery stroke it drags itself back near the wall. The recovery stroke is initiated by the propagation of a bending wave from the base to the tip of the cilium.

Proto-zoologists quite often observe that the flagella near to each other tend to synchronize their movements (see theoretical discussion in Taylor 1951). Generally in cilia the opposite observation can be made because adjacent cilia in the beating direction are out of phase and this is realized in the metachronal wave. Thus, when viewed from above the metachronal wave appears as a wave passing over the surface of the organism. In this paper we concern ourselves with two different types of metachronal wave. The first, called symplectic metachronism, occurs when the wave travels in the same direction as the effective beat. The other variety occurs when the wave travels in the opposite direction to the effective beat and is classified as antiplectic metachronism (Knight-Jones 1954). We also consider a synchronized beat when all the cilia are beating in phase, but if this happens the cycle of beating is altered considerably. We use data from three organisms as models for our theory, these being *Opalina*, which

exhibits symplectic metachronism, and *Paramecium* and *Pleurobrachia*, which show antiplectic metachronal wave patterns. Data on these organisms with respect to the cilium's beat is obtained from Sleigh's (1962, 1966, 1968) papers.

In previous models for ciliated organisms (Blake 1971*a*, *b*), we considered a model which used the concept of an 'envelope' over the undulating cilia. In this approach the individuality of the ciliary beat was replaced by the action of a wave. This method is satisfactory for organisms which exhibit symplectic metachronal wave patterns, but is inappropriate for antiplectic metachronism. In this paper, we use an approach which is suitable for both types. In antiplectic metachronism the cilia are spread out during the effective stroke, so we need to take into account the individuality of the cilium's movement. To do this, we develop a theory which models the cilia of the organism by an array of flexible long slender bodies distributed over and attached at one end to a plane surface. The slender bodies are constrained to move in a similar pattern to the cilia of the micro-organisms (i.e. using an approximation employing numerical techniques). The velocity field is represented by a distribution of singularities along the axis of the slender body. A method of obtaining this singularity and the resulting interpretation of the solution can be found in Blake (1971*c*). The far-field solutions are of fundamental importance in understanding the movement of cilia.

Before we can define the relevant equations of motion a discussion of the Reynolds numbers for the movement of a cilium (R_c) and the organism (R_b) is needed. Thus we define

$$R_c = \sigma L r_0/\nu, \quad R_b = U\mathscr{L}/\nu, \tag{1}$$

where σ is the average angular frequency, L the length and r_0 the characteristic radius of the cilium, U the velocity of propulsion and $\mathscr{L}$ the length of the organism, and ν is the kinematic viscosity. In this paper we consider an infinite planar model of the organism so R_c is the only relevant Reynolds number. Because of the small length scales in protozoa ($L \sim 10\,\mu$m, $r_0 \sim 0{\cdot}1\,\mu$m) the cilium Reynolds number R_c is very small, of $O(10^{-2}$ to $10^{-6})$, for many small micro-organisms. However, in some micro-organisms the beat fequency f (where $\sigma = 2\pi f$) may be high so the cilium Reynolds number R_c may approach one, while in the Ctenophores ('comb bearers'), where many cilia combine together ($O(10^5)$ cilia) to form a combplate, the resulting Reynolds number for the combplate may be greater than one (a combplate may be $800\,\mu$m in length and $500\,\mu$m in width with a beat frequency around $20\,\mathrm{s}^{-1}$ which would give $R_c \sim 10$–20).

Thus, in many micro-organisms the Reynolds number is small enough to justify using the creeping-flow equations, defined as follows:

$$\nabla p = \mu \nabla^2 \mathbf{q}, \quad \nabla . \mathbf{q} = 0, \tag{2}$$

where p is the pressure, $\mathbf{q}$ the velocity vector and μ the dynamic viscosity. The shape and movement of the cilium during its beat suggests that a 'Stokeslet' distribution (and the associated image, i.e. the Green's function obtained from (2)) along the centre-line can be employed. The cilium tends to beat in a near rigid-body movement in its effective beat and then drags itself back through the

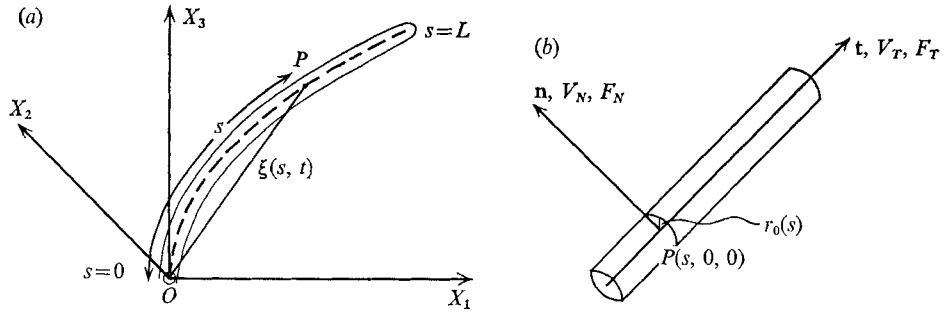

FIGURE 1. Diagrams illustrating the co-ordinate representations for a cilium: (*a*) Cartesian co-ordinates for $\xi(s, t)$; (*b*) the local 'inner' co-ordinates, where **t** is the tangent and **n** is the normal to the centre-line. The radius of the cilium at P is $r_0(s)$.

fluid to the beginning of its effective beat again. Hancock (1953) showed that the movement of an infinite cylinder perpendicular to its axis is twice as effective in producing 'general motion' as moving the cylinder parallel to itself (i.e. along its axis). This classic paper of Hancock's was used to obtain the velocity of propulsion for spermatozoa in an infinite viscous fluid. As a result of this work, Gray & Hancock (1955) wrote a paper using simple dynamical arguments to obtain the velocity of propulsion of sea-urchin spermatozoa with remarkable accuracy. This paper became the forerunner of many similar papers on flagella and cilia motion (see, for example, Holwill 1966; Holwill & Sleigh 1967*b*; Brokaw 1970).

Barton & Raynor (1967) use a model for a cilium in their paper on motion of mucus in the trachea. They take the cilium to be a rigid rod rotating about its base which automatically shortens for the recovery stroke. A distribution of these rods is then made over a plane boundary, with no account being taken of the metachronal wave over the surface of the sheet of cilia. There are several features of their paper which we wish to improve upon: some of these being an accurate representation of the movement of a cilium, the influence of the wall on the far field, inclusion of the metachronal wave and interaction between the cilia.

2. Single cilium

For our discussion of the velocity field due to a single cilium, we suppose that a long slender body, representing the cilium, has its base attached to an infinite planar surface (X_1OX_2 plane). Axes are taken fixed in the organism. We assume that the slender body is essentially cylindrical, of radius $r_0(s)$, where s measures the distance along the centre-line of the cilium from its base (the origin in figure 1). Although we have taken the cross-section of the cilium to be cylindrical, it could be altered to include a flat-plate cross-section (e.g. to take into account the combplates of some Ctenophores) by extending the approach of Batchelor (1970) for non-cylindrical cross-sections. The length of the cilium is taken to be L, so that $0 \leqslant s \leqslant L$, while the position of a point P on the cilium centre-line

is designated in Cartesian co-ordinates by $\boldsymbol{\xi}(s,t)$ (a Lagrangian formulation in distance s and time t).

The introduction of a distribution of singularities along the centre-line is a simplification that is often made when we are considering long slender bodies. Ladyzhenskaya (1963) showed that an exact and unique solution exists for Stokes flow if a surface distribution of singularities is used. We assume that this can degenerate into a distribution of Stokeslets, Stokes-doublets and higher singularities along the centre-line of a long slender body (see Tuck (1968), Batchelor (1970) and Tillett (1970) for a further discussion).

The singularities needed for this model are required to satisfy the no-slip condition on the surface of the plane boundary. Thus, the equations and boundary conditions defining this singularity (Green's function) are as follows:

$$\left.\begin{aligned} \nabla p &= \mu\nabla^2\mathbf{u}+\mathbf{F}\delta(\mathbf{x}-\boldsymbol{\xi}),\\ \nabla.\mathbf{u} &= 0,\\ \mathbf{u} &= 0 \quad \text{on} \quad x_3 = 0, \end{aligned}\right\} \tag{3}$$

where p is the pressure, μ the viscosity, $\mathbf{u}$ the velocity vector, $\mathbf{F}$ the force and $\delta(\mathbf{x}-\boldsymbol{\xi})$ the Dirac delta function. We define the Green's function and velocity as follows:

$$\begin{aligned} u_j(\mathbf{x}) &= F_k G_j^k(\mathbf{x},\boldsymbol{\xi})\\ &= \frac{F_k}{8\pi\mu}\left[\left\{\frac{\delta_{jk}}{r}+\frac{r_j r_k}{r^3}\right\}-\left\{\frac{\delta_{jk}}{R}+\frac{R_j R_k}{R^3}\right\}\right.\\ &\qquad \left.+2\xi_3(\delta_{k\alpha}\delta_{\alpha l}-\delta_{k3}\delta_{3l})\frac{\partial}{\partial R_l}\left\{\frac{\xi_3 R_j}{R^3}-\left(\frac{\delta_{j3}}{R}+\frac{R_j R_3}{R^3}\right)\right\}\right], \end{aligned} \tag{4}$$

where $\alpha = 1$ or 2, and r and R are defined as follows:

$$r = [(x_1-\xi_1)^2+(x_2-\xi_2)^2+(x_3-\xi_3)^2]^{\frac{1}{2}}$$

and

$$R = [(x_1-\xi_1)^2+(x_2-\xi_2)^2+(x_3+\xi_3)^2]^{\frac{1}{2}},$$

the coefficients r_i and R_i being apparent from these definitions. The other singularities, apart from the initial Stokeslet (the r_i terms), are a Stokeslet, Stokes-doublet and a source-doublet situated at the image point $(\xi_1, \xi_2, -\xi_3)$. Equation (4) can be obtained from Oseen (1927) for the movement of a sphere near a wall at very low Reynolds number. A discussion of an alternative method for obtaining this singularity and an interpretation of the result is given in Blake (1971*c*). It is shown that the far field for a point-force singularity has a Stokes-doublet (stresslet) character for a force parallel to the plane. In the other case, for a force perpendicular to the plane boundary, the far field is a combination of a Stokes-quadrupole and a source-doublet, which is a higher order singularity than for the case of a force parallel to the plane.

The total velocity field due to a single cilium can now be expressed in terms of the following integral equation:

$$u_j(\mathbf{x}) = \int_0^L F_k[\boldsymbol{\xi}(\hat{s},t)]\, G_j^k(\mathbf{x},\boldsymbol{\xi}(\hat{s},t))\, d\hat{s}, \tag{5}$$

where $F_k[\xi(s,t)]$ is the functional representation for the force distribution along the slender body.

We define the velocity at the surface of the cilium, which corresponds to $(s, r_0(s), \phi)$ $(0 \leqslant \phi < 2\pi)$ in the 'inner' co-ordinates, by applying the no-slip condition

$$U_i^* = \partial \xi_i / \partial t \quad (i = 1, 2, 3). \tag{6}$$

Therefore we can equate U_i^* to the integral (5), thus defining an inverse problem for the force **F**. This is extremely difficult to solve as we need to take into account interaction effects with other cilia and the influence of the wall. Further discussion on calculations for the force are made in § 4.

A force singularity of strength F_α $(\alpha = 1, 2)$, acting in the x_α direction at (ξ_1, ξ_2, ξ_3) a distance ξ_3 above the plane, induces the following far-field effects (i.e. stresslet) on the velocity:

$$u_i \sim \frac{12 \xi_3 F_\alpha}{8\pi\mu} \frac{r_i^* r_\alpha^* r_3^*}{r^{*5}} + O\left(\frac{1}{r^{*3}}\right), \tag{7}$$

where

$$r^* = [(x_1 - \xi_1)^2 + (x_2 - \xi_2)^2 + x_3^2]^{\frac{1}{2}},$$

the form of components r_i^* being obvious from this definition. The $\xi_3 F_\alpha$ term in (7) can be interpreted as a 'first moment' type term. The error terms in (7) consist of higher singularities (e.g. $\xi_3 \xi_i F_j$; $i, j = 1, 2, 3$) or 'moments' of the form $\xi_3 F_3$ (i.e. Stokes-quadrupole terms).

Thus the velocity in the far field due to a single cilium at the origin can be written as

$$u_i \sim \frac{3 r_3^*}{2\pi\mu} \int_0^L \frac{r_i^* r_\alpha^*}{r^{*5}} \xi_3 F_\alpha \, d\hat{s} + O\left(\frac{1}{r^{*3}}\right), \tag{8}$$

where the components r_i^* are defined in (7). To include the influence of all the cilia we need to sum the velocities over an array of similar slender bodies.

A physical interpretation of the movement of a cilium in terms of near- and far-field influences can be given. We can approximate the region around the force singularity, which has a Stokeslet ($O(1/r)$) velocity field, by a sphere of radius $\frac{1}{2}\xi_3$. This means that during the effective stroke the cilium influences a relatively large volume of fluid with its Stokeslet field (see figure 2(*a*)) in comparison with its movement in the recovery stroke, when only the region in the close proximity of the cilium is influenced by the near field (figure 2(*b*)). Furthermore, one can extend this to a row of cilia in different stages of their beat. The Stokeslet region influenced by the effective beat consists of the upper half of the ciliary sublayer, while only the lower part feels the recovery stroke. Thus one might anticipate the oscillatory component of the velocity to be small in relation to the mean flow in the upper half of the cilia sublayer. Conversely, the oscillatory component can be quite large in comparison with the mean flow in the lower part of the sublayer (figure 2(*c*)).

A further feature contributing to the large effective stroke Stokeslet region is that the force is larger during the effective stroke in antiplectic metachronism. This is due to two factors, one being the larger relative velocities of the effective

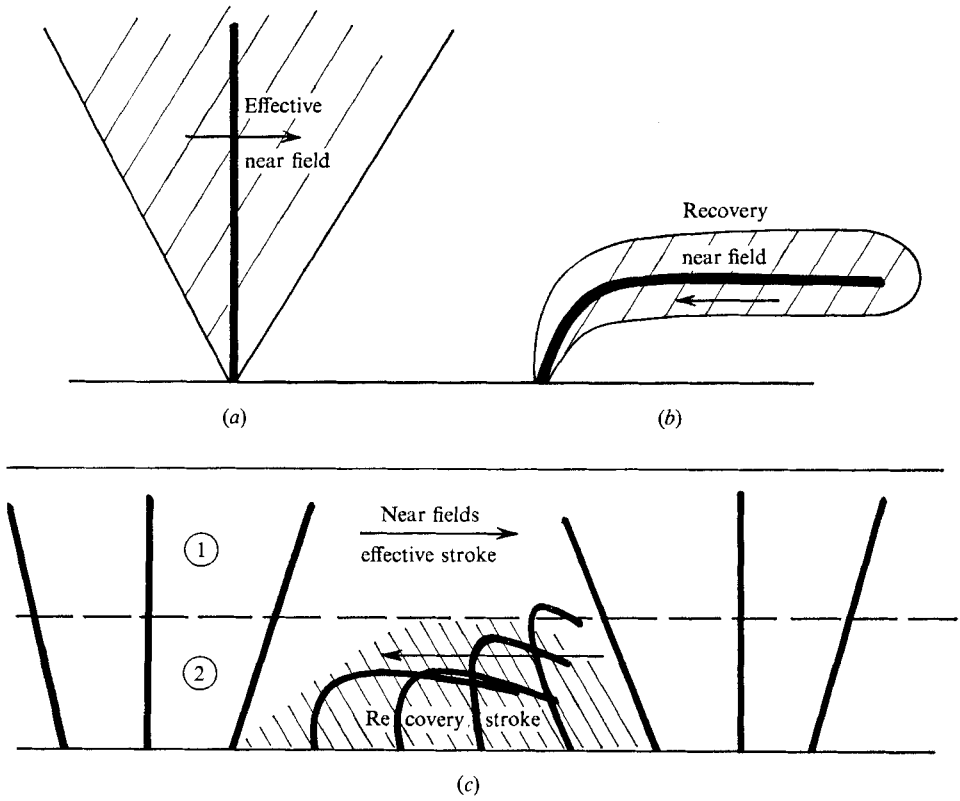

FIGURE 2. (*a*) The Stokeslet near field during the effective stroke of a cilium; (*b*) Stokeslet field during recovery stroke; and (•) the relative near fields in a wave of beating cilia. In region ① the fluid is influenced mainly by the effective stroke while in ② it is influenced equally by both movements.

stroke, the other being the fact that a slender body exerts nearly twice the force (for a given velocity) if it moves normally instead of tangentially.

Thus, we have two reasons why a cilium moves in a near rigid-body motion in its effective stroke, and close to the wall during the recovery movement, these being the near-field influences on the fluid and the force exerted in each phase of the beat.

Experimentally it is observed (Sleigh & Aiello 1971) that the oscillatory component is small in the uppermost part of the sublayer; however, further experimental work needs to be carried out in the lower regions of the cilia sublayer. This has a rather interesting effect on the mean velocity profiles which are discussed in a later section.

3. Array of cilia

Let us consider a regular array of cilia bases on the infinite plane $x_3 = 0$, with spacing a in the x_1 direction and b in the x_2 direction (see figure 3). The effective stroke of the ciliary beat will be taken in the direction of increasing x_1,

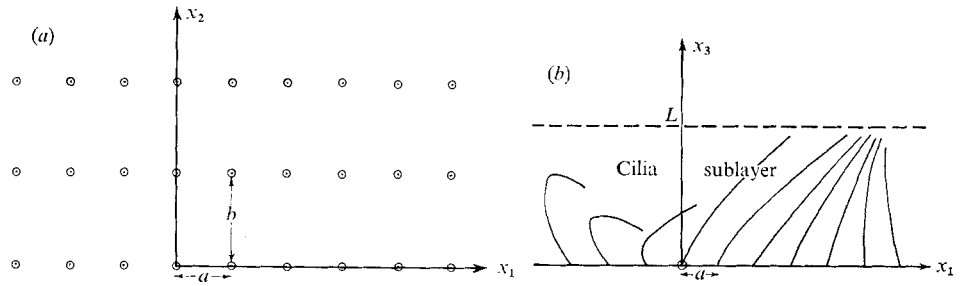

FIGURE 3. Illustrations of regular array of cilia: (*a*) from above and (*b*) side-on view for symplectic and antiplectic metachronism. The spacing in the x_1 direction is a, while in the x_2 direction it is b.

although it need not be a planar beat. We suppose the wave crests of the metachronal wave are parallel to the x_2 axis, that is, we are modelling either anti- or simplectic metachronism. The strength of the force singularity distribution **F** will be equal along lines parallel to the x_2 axis, but variable in the x_1 direction. The justification for this approach is that organisms exhibiting symplectic or antiplectic metachronism are generally elongated or flat so the approximation of using an infinite plane is plausible. However, in the other types of metachronism cilia tend to be in short rows so this model cannot be used.

We need a general formulation for the movement of a cilium so that it can move freely. This is desirable because organisms such as *Paramecium* clearly have a beat three-dimensional in form. To model the metachronal wave described above and the movement of a cilium at the general point (ma, nb) on the X_1OX_2 plane we define

$$\xi_1' = x_1 + \xi_1(s,\tau), \quad \xi_2' = x_2 + \xi_2(s,\tau), \quad \xi_3' = \xi_3(s,\tau), \tag{9}$$

where $x_1 = ma$, $x_2 = nb$ and $\tau = kx_1 \pm \sigma t$. We now have a model for the metachronal wave which has a velocity $c = \sigma/k$, wavelength $2\pi/k$ and frequency $\sigma/2\pi$. Thus the positive sign is used to model antiplectic metachronism while the negative sign models symplectic metachronism.

The total bulk velocity field in terms of all the slender bodies distributed in an array over an infinite plane can be represented in terms of the following infinite double summation:

$$u_j(\mathbf{x},t) = \sum_{n=-\infty}^{\infty} \sum_{m=-\infty}^{\infty} \int_0^L F_k[\boldsymbol{\xi}'] G_j^k(\mathbf{x},\boldsymbol{\xi}')\, d\hat{s}, \tag{10}$$

with F_k, G_j^k and $\boldsymbol{\xi}'$ all being defined previously. This does not allow us to say anything about the local flow properties of the cilium (e.g. the flat combplates of the Ctenophores tend to 'capture' some particles, especially near their base). The velocity field of most interest to us is the mean field, so we define

$$\mathbf{u} = \mathbf{U} + \mathbf{u}', \quad \text{where} \quad \mathbf{U} = \bar{\mathbf{u}}, \tag{11}$$

with the bar over the velocity symbol implying the time mean. Because of the path of movement of a cilium we would expect $|\mathbf{u}'|$ to be considerably less than $|\mathbf{U}|$ in a region $x_3 > \delta$, where $\delta < \frac{1}{2}L$, L being the length of the cilium (see figure 2).

Equation (10) is difficult to evaluate, but it may be simplified if we take both a time and a spatial average in the x_1, x_2 plane. To improve the convergence of the double sum we apply the Poisson summation formula, which employs the Fourier-transformed double sum (see, for example, Lighthill 1958, p. 67; Jones 1966, p. 276). The transformed sum now becomes a decreasing exponential infinite series, so for an approximation we consider only the zeroth term, an estimation being obtained for the error. Thus on evaluation we obtain

$$\left.\begin{aligned} U_\alpha(x_3) &= \frac{1}{\mu ab}\overline{\int_0^L w(\hat{s},t)\,K(x_3,\xi_3)\,F_\alpha[\hat{\boldsymbol{\xi}}]\,d\hat{s}} + O(ab/L^2)\,\sigma L \quad (\alpha = 1,2),\\ U_3(x_3) &= O(ab/L^2)\,\sigma L, \end{aligned}\right\} \tag{12}$$

where $K(x_3, \xi_3)$, the 'kernel' function, is obtained by spatially integrating $\mathbf{G}$ over the X_1OX_2 plane and is given by

$$\begin{aligned} K(x_3,\xi_3) &= \tfrac{1}{2}[x_3 + \xi_3 - |x_3 - \xi_3|]\\ &= \begin{cases} x_3 & (x_3 < \xi_3),\\ \xi_3 & (x_3 > \xi_3). \end{cases} \end{aligned} \tag{13}$$

The weight function $w(s,t)$, obtained from the Jacobian in the integration, is defined by

$$w(s,t) = \left\{\begin{array}{l} 1 \quad : \text{synchronized},\\ \dfrac{1}{1-(1/c)\,\partial\xi_1/\partial t} : \text{symplectic},\\ \dfrac{1}{1+(1/c)\,\partial\xi_1/\partial t} : \text{antiplectic}. \end{array}\right\} \tag{14}$$

For the integral to be non-singular we need

$$1 \pm \frac{1}{c}\frac{\partial \xi_1}{\partial t} > 0 \;\forall\; s \in (0, L), \tag{15}$$

and throughout the beat because to evaluate the sum we need to replace the discrete system by a continuum. However, since cilia are discrete identities they need not obey this constraint and often do not. In many organisms exhibiting antiplectic metachronism, the ciliary beat is a three-dimensional motion, so the above restriction may be avoided. Generally $ab \ll L^2$ so the approximation is a reasonable one.

We turn to a physical interpretation of the kernel function $K(x_3, \xi_3)$. From Blake (1971*c*) we know that the only contribution to the force integral (in terms of the stress) comes from the plane surface which lies between the singularity and the stationary plane boundary, the contribution from the hemisphere at infinity being zero. Thus, if we consider a spatial average, in the x_1, x_2 plane, of the velocity field for a force F'_α per unit area on the plane $x_3 = \xi_3$ (even though the force distribution may be at discrete points) we obtain

$$\left.\begin{aligned} F'_\alpha &= \mu\, dU_\alpha/dx_3 \quad \text{for} \quad x_3 < \xi_3\\ 0 &= \mu\, dU_\alpha/dx_3 \quad \text{for} \quad x_3 > \xi_3 \end{aligned}\right\} \quad (\alpha = 1,2). \tag{16}$$

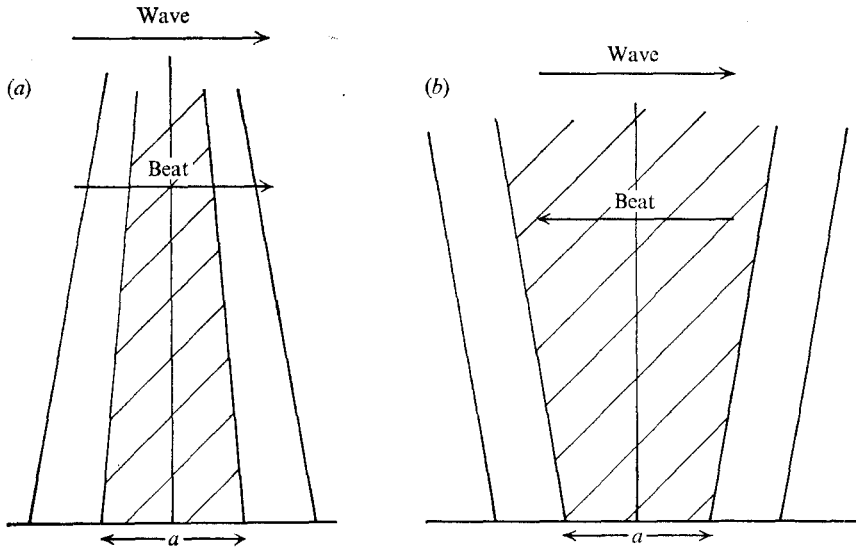

FIGURE 4. The shaded region indicates the altered averaging area in the effective beat for (*a*) symplectic and (*b*) antiplectic metachronism.

Averaging area	Symplectic ($\sigma_e = \sigma_r$)	Antiplectic ($\sigma_e = 3\sigma_r$)
Effective	$1-\sigma L/c$	$1+2\sigma L/c$
Recovery $\xi < \frac{1}{2}L$	$1+\frac{1}{2}\sigma L$	$1-\frac{1}{3}\sigma L/c$

This, when integrated, yields

$$U_\alpha(x_3) = (1/\mu)\, F'_\alpha K(x_3, \xi_3). \tag{17}$$

This is what we would expect from the Stokes-flow equations, in the absence of a pressure field, because the only allowable velocity field is that of shear flow between the two planes and a constant streaming above.

The velocity U^∞_α ($\alpha = 1, 2$) of propulsion of the infinite sheet, which can be obtained from either (12) or by summing the far fields of all the cilia (see equation (8)), is

$$U^\infty_\alpha = (1/\mu)\, \bar{S}_\alpha \quad (\alpha = 1, 2),$$

with

$$S_\alpha = \frac{1}{ab}\int_0^L \omega(\hat{s}, t)\, \xi_3(\hat{s}, t)\, F_\alpha[\hat{\boldsymbol{\xi}}]\, d\hat{s}, \tag{18}$$

where $\bar{S}_\alpha$ is the time-averaged stresslet strength per unit area. The weight function $\omega(s, t)$ takes into account the metachronal wave. It alters the 'averaging area' from ab to $ab\omega^{-1}(s, t)$ because of the influence of the wave. The term $(1/c)\, \partial\xi_1/\partial t$ is the ratio of the cilium's x_1 velocity to the metachronal wave speed. To gain some idea of the magnitude of this ratio we define two angular frequencies which correspond to the effective and recovery strokes. Thus, we define

$$\sigma = 2\sigma_e\sigma_r/(\sigma_e + \sigma_r), \tag{19}$$

where σ is equal to the average angular frequency and σ_e and σ_r are equal to the effective and recovery angular frequencies respectively. In figures 4 (*a*) and (*b*) we illustrate the averaging areas for the 'basic element' ab during the effective strokes for both symplectic and antiplectic metachronism. It is obvious from

figure 4(*a*) that during the effective stroke in symplectic metachronism the cilia are close together, whereas in antiplectic metachronism the cilia are spread out. In the recovery stroke the opposite occurs, but in this case the cilia are moving much more slowly, especially in antiplectic metachronism (for symplectic metachronism $\sigma_e/\sigma_r \sim 1$, for antiplectic metachronism $2 \lesssim \sigma_e/\sigma_r \lesssim 3$) and in a region $x_3 < \frac{1}{2}L$, so the weight functions $w(s,t)$ will be near 1.

We can make some general observations about the stresslet strength S_α ($\alpha = 1, 2$). This function of time takes on both positive and negative values depending on the stage of the beat of a cilium. It is apparent from (18) that to maximize the mean of S_α over a cycle would be to have S_α as large as possible in the effective stroke and as small as possible (in magnitude) during the recovery stroke. This is one reason why cilia tend to rotate like rigid rods in the effective stroke ($0 \leqslant \xi_3 \leqslant L$) and retreat 'limply' near the wall during the recovery stroke ($0 \leqslant \xi_3 \leqslant \frac{1}{2}L$). Obviously there are many other physical effects governing the motion of a cilium, but we leave these to a further discussion after the force F_α has been obtained. There are many variations in the movement of cilia from organism to organism; this is due to the varying physical situations and the associated biological optimization of the movement, function, energy expenditure, etc.

From this discussion it follows that the drag D_α of the 'basic element' ab which contains the cilium is

$$D_\alpha = -\mu ab \overline{\left[w^{-1}(s,t) \frac{\partial U_\alpha}{\partial x_3} \right]}_{x_3=0}$$

$$= -\int_0^L \overline{F_\alpha[\hat{\boldsymbol{\xi}}]}\, d\hat{s}. \tag{20}$$

Thus

$$D_\alpha + \int_0^L \overline{F_\alpha[\hat{\boldsymbol{\xi}}]}\, d\hat{s} = 0,$$

which indicates that the sum of the force exerted by a cilium in one cycle and the drag of its 'basic element' of area ab is equal to zero. This is what we would expect from the general principle that the force exerted by a micro-organism is zero. In the envelope approach (Blake 1971*a*, *b*), we used this principle to eliminate the 'Stokeslet' terms in our expression for the velocity fields.

4. Force exerted by a cilium

In this section we evaluate the force exerted by a cilium as a function of its movement $\boldsymbol{\xi}$ and include the influence of nearby cilia. The problem of a curved slender body in an infinite viscous fluid has been treated previously by Hancock (1953) and Cox (1970, 1971).

We could use either approach to the problem. Cox's asymptotic expansion for the force **F**, which is a formal, mathematically valid expansion, is a little unwieldly. The approach derived from Hancock, as illustrated in the paper of Gray & Hancock (1955), is perhaps more suited to this problem. We shall use a combined theory employing features from both papers. Another method that may have some applications to this type of problem is that of Batchelor (1971)

for 'concentrated' distributions of slender bodies. In this analysis, we shall assume that the cilia are relatively spread out, at least during the effective stroke, when they are exerting their largest force (e.g. in antiplectic metachronism – *Paramecium* and *Pleurobrachia*), so the modified method of Gray & Hancock will be used. From the linearity of the creeping-flow equations, we can write down the element force $\delta\mathbf{F}$ in terms of the tensor A_{ij} as

$$\delta F_i = \mu A_{ij} v_j \delta s, \tag{21}$$

where v_j is the velocity of the body relative to the fluid.

The Gray & Hancock (1955) technique is based on the simple dynamical assumption that, when it moves through the viscous fluid, each infinitesimal element of the cylinder exerts a normal and tangential force which is proportional to the velocities in these directions (i.e. equation (21)). Gray & Hancock used the solution for the case of an infinite cylinder when the ratio of the coefficients of the velocities in these two forces (i.e. $\gamma = C_N/C_T$) is two. However, it is found (Hancock 1953; Tillett 1970; Batchelor 1970) that for a finite slender body γ is less than two, having an asymptotic expansion in terms of the slenderness coefficient of the body. The expansion for γ (Tillett 1970) for a straight slender body in an infinite viscous fluid is

$$\gamma = 2 - \frac{2}{\log(L/r_0)} + O\left(\frac{1}{[\log(L/r_0)]^2}\right), \tag{22}$$

which if applicable to cilia indicates a range of γ from 1·6 to 1·9.

If we take the force distribution exerted by the cilium on the fluid at the point P, we can develop the following representation for the normal and tangential force due to the movement of the cilium. δF_N and δF_T are the normal (along $\mathbf{n}$) and tangential (along $\mathbf{t}$) force elements and V_N and V_T the normal and tangential velocities respectively (the normal $\mathbf{n}$ is chosen such that the binormal component of the velocity is zero).

The forces which the cilium exerts on the fluid may be written down in terms of the local fluid velocity $\mathbf{v}$ as

$$\left.\begin{aligned} \delta F_T &= C_T V_T \delta s = C_T(\mathbf{v}.\mathbf{t})\,\delta s, \\ \delta F_N &= C_N V_N \delta s = C_N(\mathbf{v}.\mathbf{n})\,\delta s, \end{aligned}\right\} \tag{23}$$

where C_N and C_T are the normal and tangential force coefficients and are defined as follows:

$$C_T = 2\pi\mu/[\log(L/r_0) + k_1], \quad C_N = \gamma C_T, \tag{24}$$

where

$$\gamma = 2 + \frac{\alpha}{\log L/r_0} + O\left(\frac{1}{[\log(L/r_0)]^2}\right),$$

and k_1 is a constant obtained by integration over the length of the cilium (i.e. an average value). For simple shapes the constant k_1 can be easily obtained (e.g. for the straight slender body, see Cox 1970), but for the general case needed in this theory we shall content ourselves with varying it slowly and using $k_1 = O(1)$. In zoological literature k_1 is often taken equal to $\log 2 - \frac{1}{2}$ and $\gamma = 2$. C_N and C_T may be referred to as the modified Gray & Hancock coefficients. Improved values

of C_N and C_T have been formulated in a recent paper by Shack, Fray & Lardner (1971).

From (23) we can now write down the force in the original co-ordinates as

$$\delta\mathbf{F} = [C_T(\mathbf{v}.\mathbf{t})\,\mathbf{t} + C_N(\mathbf{v}.\mathbf{n})\,\mathbf{n}]\,\delta s, \tag{25}$$

with the constraint that $\mathbf{v}.\mathbf{b} = 0$. By making use of the properties of the idemfactor $\mathbf{I}$ and substituting for $\mathbf{t}\,(= \partial\boldsymbol{\xi}/\partial s)$ and C_T we obtain the following representation for the force element $\delta\mathbf{F}$ in terms of the movement of a cilium.

$$\delta\mathbf{F} = \frac{2\pi\mu}{\log(L/r_0) + k_1}\mathbf{v}.\left[\gamma\mathbf{I} - (\gamma-1)\frac{\partial\boldsymbol{\xi}}{\partial s}\frac{\partial\boldsymbol{\xi}}{\partial s}\right]\delta s. \tag{26}$$

If we took $\gamma = 2$ and $k_1 = 0$ we would generate the first approximation in the asymptotic expansion of Cox (1970).

The interaction effects of all the other cilia can be included in the velocity $\mathbf{v}$, by defining

$$\mathbf{v} = \partial\boldsymbol{\xi}/\partial t - \mathbf{u}^*, \tag{27}$$

where $\mathbf{u}^*$ is the interaction velocity field. Cox (1970) indicates that the interaction effects are of second order, which is a result of the iterative process used. We find it more convenient to use the above definition because we can then define the velocity field in terms of an integral equation.

5. Coupled integral equations for mean velocity field

We have previously defined the total velocity field as $\mathbf{u}$ and the mean velocity as $\mathbf{U}$. The interaction velocity $\mathbf{u}^*$ of (35) will be taken as

$$\mathbf{u}^* = \mathbf{U} - \mathbf{V} + \mathbf{v}', \quad \overline{\mathbf{v}'} = 0, \tag{28}$$

where $\mathbf{V}$ is the contribution of the cilium in question to the local mean velocity field. To define the coupled integral equation we will consider the mean velocity fields $\mathbf{U}$ and $\mathbf{V}$ and neglect the oscillatory variation $\mathbf{v}'$. Thus the mean velocity field U_α $(\alpha = 1, 2)$ is defined by

$$U_\alpha(x_3) = \frac{2\pi}{ab[\log(L/r_0) + k_1]}\int_0^L \overline{w(\hat{s}, t)\,K(x_3, \xi_3)} \times \overline{\left(\frac{\partial\hat{\xi}_i}{\partial t} - U_i(\xi_3) + V_i(\hat{\boldsymbol{\xi}})\right)\left(\gamma\delta_{i\alpha} - (\gamma-1)\frac{\partial\hat{\xi}_i}{\partial s}\frac{\partial\hat{\xi}_\alpha}{\partial s}\right)}\,d\hat{s} \quad (\alpha = 1, 2), \tag{29}$$

and the mean velocity field due to a single cilium is defined as follows:

$$V_i(\boldsymbol{\xi}) = \frac{2\pi\mu}{\log(L/r_0) + k_1}\int_0^L \overline{G_i^j(\boldsymbol{\xi}, \hat{\boldsymbol{\xi}})\left(\gamma_{jk} - (\gamma-1)\frac{\partial\hat{\xi}_j}{\partial s}\frac{\partial\hat{\xi}_k}{\partial s}\right)} \times \overline{\left(\frac{\partial\hat{\xi}_k}{\partial t} - U_k(\xi_3) + V_k(\hat{\boldsymbol{\xi}})\right)}\,d\hat{s}, \tag{30}$$

where $G_i^j(\boldsymbol{\xi}, \hat{\boldsymbol{\xi}})$ is the Green's function defined in (4) while $\hat{\xi}$ implies $\xi(\hat{s}, t)$. The integral equation (29) is solved by matrix inversion using an iterative process for $\mathbf{V}$ in (30).

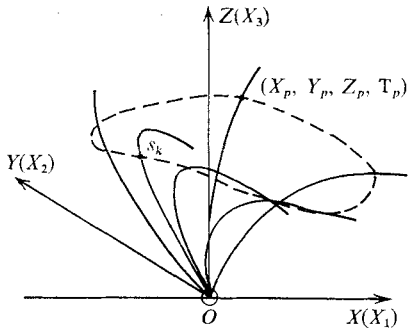

FIGURE 5. Measurements recorded in one cycle of a cilium's beat. Lagrangian point s_k along cilium. (X_p, Y_p, Z_p, T_p) specifies the point during cycle, while the dashed line indicates its path through one cycle.

6. Numerical calculations on the movement of a cilium

6.1. *Movements of a cilium*

In the prior analysis the position of each point of the cilium has only been specified by the general vector function $\boldsymbol{\xi}(s,\tau)$. In this section we define and obtain approximate analytic representations for the observed periodic beat of a cilium. The general movement of a cilium at a point (x_1, x_2) on the X_1OX_2 plane was defined in (9), although in the numerical models we take $\xi_2 = 0$ because the available data is only in a two-dimensional form.

The movement of a cilium is periodic, so we can represent ξ_i $(i = 1, 2, 3)$ by a Fourier series expansion in τ. The following measurements are records of the cilium's movement. We take K stations along the length of a cilium, denoted by s_k $(k = 1, \ldots, K)$, and at each station s_k we record the periodic movement of the cilium (X_p, Y_p, Z_p, T_p), $p = 1, \ldots, 2N+1$. (X_p, Y_p, Z_p) denotes the path the point s_k on the cilium traces out in one cycle (see figure 5). The Fourier series representation for ξ_i $(i = 1, 2, 3)$ is as follows:

$$\left.\begin{aligned}
\xi_1 &= \tfrac{1}{2}a_0(s) + \sum_{n=1}^{N} [a_n(s)\cos n\tau + b_n(s)\sin n\tau],\\
\xi_2 &= \tfrac{1}{2}c_0(s) + \sum_{n=1}^{N} [c_n(s)\cos n\tau + d_n(s)\sin n\tau],\\
\xi_3 &= \tfrac{1}{2}f_0(s) + \sum_{n=1}^{N} [f_n(s)\cos n\tau + g_n(s)\sin n\tau],
\end{aligned}\right\} \tag{31}$$

where $a_n(s)$, $b_n(s)$, $c_n(s)$, $d_n(s)$, $f_n(s)$ and $g_n(s)$ are polynomial functions of s, determined by a least-squares fit. The Fourier series coefficients $a_n^k, b_n^k, \ldots$ are obtained at each point s_k and the polynomials $a_n(s), b_n(s), \ldots$ are then obtained by a least-squares fit to the coefficients. Thus,

$$a_n(s) = \sum_{m=1}^{M} A_{mn}s^m, \quad b_n(s) = \sum_{m=1}^{M} B_{mn}s^m, \quad \ldots. \tag{32}$$

There are no constant in terms in the polynomaial expansion because $\xi_i(0,\tau) = 0$ $(i = 1, 2, 3)$.

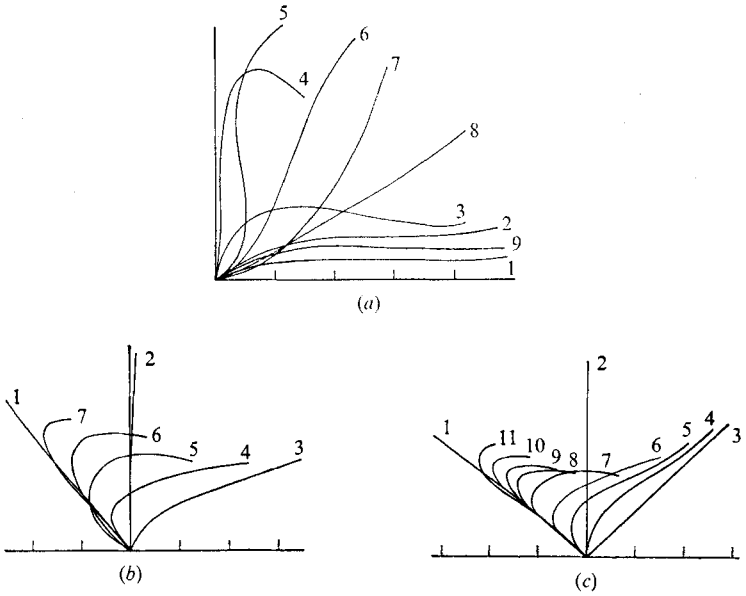

FIGURE 6. The Fourier-series–least-squares models for (*a*) *Opalina*, (*b*) *Paramecium* and (*c*) *Pleurobrachia*. Numbers indicate successive stages of the beat. The effective stroke in *Opalina* is from 5 to 9, in *Paramecium* is from 1 to 3 and in *Pleurobrachia* from 1 to 3.

Calculations were carried out on data obtained from three organisms, namely *Opalina*, *Paramecium* and *Pleurobrachia* (Sleigh 1968). The data was obtained by freehand sketching of the diagrams of Sleigh, so the data are not particularly accurate. Further inaccuracy occurs for the case of *Paramecium*, where the cilium's beat is plainly three-dimensional, but no reliable data are available on its three-dimensional movement. *Pleurobrachia* probably contravenes the low Reynolds number assumption, but on the other hand the best available data that we have are on this organism.

The Fourier-series–least-squares process was used with $N = 3$ for *Paramecium*, $N = 4$ for *Opalina* and $N = 5$ for *Pleurobrachia* with $M = 3$ in all cases. The data were collected at 10 points along the cilium (excluding the origin). In figure 5 we see the approximate analytic representation for the movement of the cilia. It appears to be reasonably accurate except in regions of high curvature. It may be argued that it is pointless to obtain the least-squares fit to the cilium's movement where a direct numerical approach would be more appropriate. We prefer the present approach because of the inadequacies of the data, so that in the following calculations the gradients used will be analytic values obtained from the Fourier–least-squares fit described in (31). At any rate we can compare the movements illustrated in figure 6 with the calculations for the velocity fields and force and bending moments shown in figures 7 and 10.

6.2. *Mean velocity field*

To find the mean velocity field in the cilia sublayer we need to resort to numerical techniques. The best way to solve the integral equation in (29) is by the matrix equation approach. Thus if we non-dimensionalize the integrals (29) and (30)

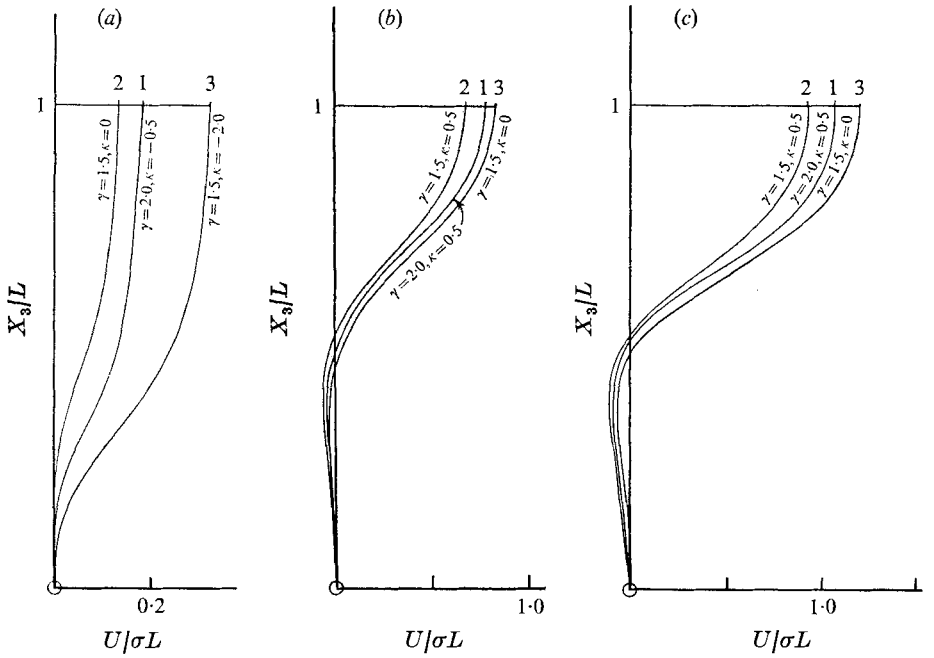

FIGURE 7. Mean velocity profiles for (*a*) *Opalina*, (*b*) *Paramecium* and (*c*) *Pleurobrachia*. The profiles are taken at T = 150. To give an indication of the variations of U with γ, κ and T we present the following table (tip speed of cilium $\sim$ 1–1·5σL for (*a*) and 2–3σL for (*b*) and (*c*)).

	Symplectic	Antiplectic
Increase γ	Increases U	Increases U
Increase T	Increases U	Increases U
Increase κ	Increases U	Decreases U

for the velocities U_α and V_i with respect to σL and the length dimensions with respect to L, we obtain the following non-dimensional parameters:

$$\kappa = \frac{\sigma L}{c}, \quad \mathrm{T} = \frac{2\pi L^2}{ab[\log(L/r_0)+k_1]}. \tag{33}$$

T is generally quite large (i.e. 10–300), while $|\kappa| < 2$–3. The integral equations may now be written as

$$U_\alpha(x_3) + \mathrm{T}\int_0^1 \overline{\frac{K(x_3,\xi_3)}{1\pm\kappa\,\partial\xi_1/\partial t} U_i(\hat{\xi}_3)\left(\gamma\delta_{i\alpha}-(\gamma-1)\frac{\partial\hat{\xi}_i}{\partial s}\frac{\partial\hat{\xi}_\alpha}{\partial s}\right)}\,d\hat{s}$$
$$= \mathrm{T}\int_0^1 \overline{\frac{K(x_3,\xi_3)}{1\pm\kappa\,\partial\xi_1/\partial t}\left(\frac{\partial\hat{\xi}_i}{\partial t}+V_i(\hat{\boldsymbol{\xi}})\right)\left(\gamma\delta_{i\alpha}-(\gamma-1)\frac{\partial\hat{\xi}_i}{\partial s}\frac{\partial\hat{\xi}_\alpha}{\partial s}\right)}\,d\hat{s} \tag{34}$$

and

$$V_i(\boldsymbol{\xi}) = \frac{2\pi\mu}{\log(L/r_0)+k_1}\int_0^1 \overline{G_i^j(\boldsymbol{\xi},\hat{\boldsymbol{\xi}})\left(\gamma\delta_{jk}-(\gamma-1)\frac{\partial\hat{\xi}_j}{\partial s}\frac{\partial\hat{\xi}_k}{\partial s}\right)}\,\overline{\left(\frac{\partial\hat{\xi}_k}{\partial t}-U_k(\hat{\xi}_3)+V_k(\hat{\boldsymbol{\xi}})\right)}\,d\hat{s}, \tag{35}$$

where $G_i^j(\boldsymbol{\xi},\hat{\boldsymbol{\xi}})$ is the Green's function defined in (4).

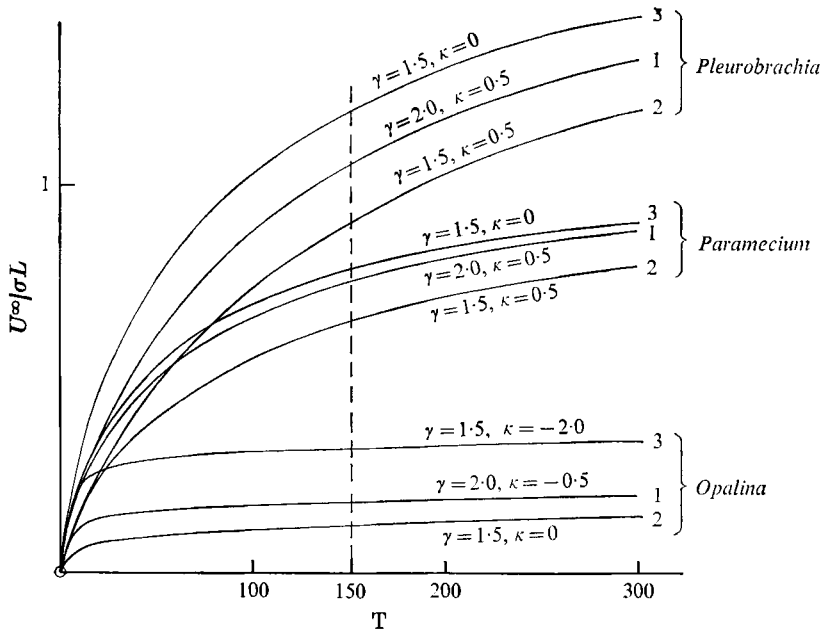

FIGURE 8. Variation of the velocity of propulsion U^∞ with T for values of γ and κ corresponding to those in figure 7 (numbered 1, 2, 3). - - - -, value of T used in figure 7.

The numerical technique used for solving (34) and (35) was to start with $V_i = 0$ in (34) and obtain a first approximation to U_α which was then substituted into (35) to obtain the first iterated value of V_i. This was then resubstituted into (34) to obtain an improved value for U_α. The rationale behind this iterative technique is that U_α is of $O(1)$, whereas V is of $O(1/\log(L/r_0))$, which is a smaller order of magnitude. In this numerical procedure we are left with three arbitrary constants which we can vary. These are γ, κ and T and the influence of these is shown in the diagrams.

In figure 7 we have shown the mean velocity fields through the cilia sublayer for our three modelled organisms. In antiplectic metachronism we observe that backflow about one tenth of the flow at the top of the sublayer is found to occur near the base of the cilia. In symplectic metachronism there was no observable backflow. To illustrate the variation of the mean flow field with respect to the arbitrary constants γ, κ and T we shall use the table shown under figure 7.

On figure 7 we have chosen varying values for both γ and κ at constant T = 150. In figure 8 we have plotted the velocity at the top of the cilia sublayer against T for several values of γ and κ corresponding to those in figure 7. Because of the numerical technique used this velocity is equal to

$$U^\infty = \alpha(\mathrm{T})\,\mathrm{T}/(1+\beta(\mathrm{T})\,\mathrm{T}), \tag{36}$$

where $\alpha(\mathrm{T})$ and $\beta(\mathrm{T})$ are rational functions of T such that

$$\lim_{\mathrm{T}\to\infty}\alpha(\mathrm{T}) = \alpha_0 \quad \text{and} \quad \lim_{\mathrm{T}\to\infty}\beta(\mathrm{T}) = \beta_0,$$

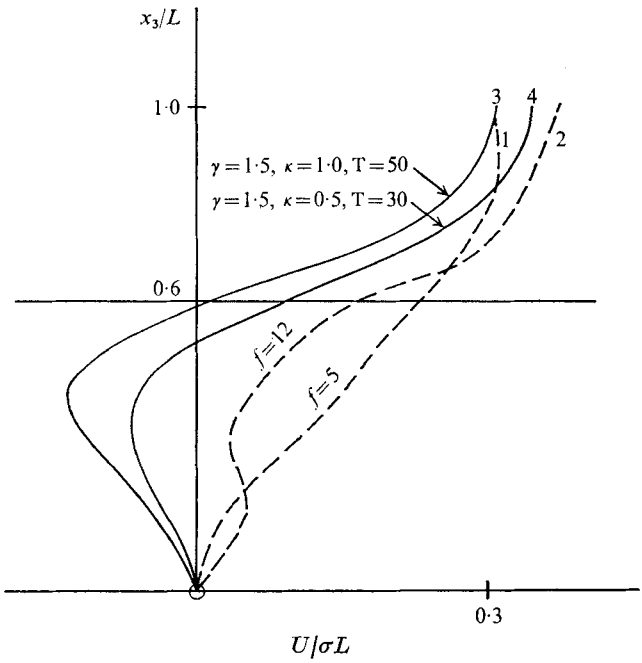

FIGURE 9. Comparisons between experiment and theory for the mean velocity field in *Pleurobrachia*. ——, theoretically predicted profiles; - - - - -, profiles observed experimentally (Sleigh & Aiello 1971). 1 corresponds to the combplate beating with a frequency of 5 beats/s (although intermittently) while the profile in 2 is for a frequency of 12 beats/s.

so that
$$\lim_{\mathrm{T}\to\infty} U^{\infty} = \alpha_0/\beta_0. \tag{37}$$

This is clearly indicated by the asymptotic nature of the graphs in figure 8.

Comparisons with experimental observations are difficult because little work has been done in this field to the author's knowledge. We would expect the above theory to be reasonably valid in *Opalina* and *Paramecium* if they exhibited the two-dimensional beat used in the calculations. However, the only known observations are those of Sleigh & Aiello (1971) on *Pleurobrachia*. We do not expect our theory to be particularly appropriate on two counts: because the Reynolds number is probably greater than one and the slender-body theory is violated. Even with these difficulties we have included calculations of *Pleurobrachia*.

For reasonable values of γ, κ and T the comparisons between experiment (Sleigh & Aiello 1971) and theory are shown in figure 9. As an estimation for γ and T we can use the values of the drag for a disk moving broadside on and edgewise (Lamb 1932), which would give $\gamma = 1{\cdot}5$ and $\mathrm{T} = \frac{32}{3}L^2/ab$. The ratio L^2/ab is of $O(1)$. The diagram shows reasonable agreement between theory and experiment above $x_3 > 0{\cdot}6$ even with all the associated difficulties. Below this level observations are not particularly accurate anyway, so there is room for improvement in both the theoretical and experimental work.

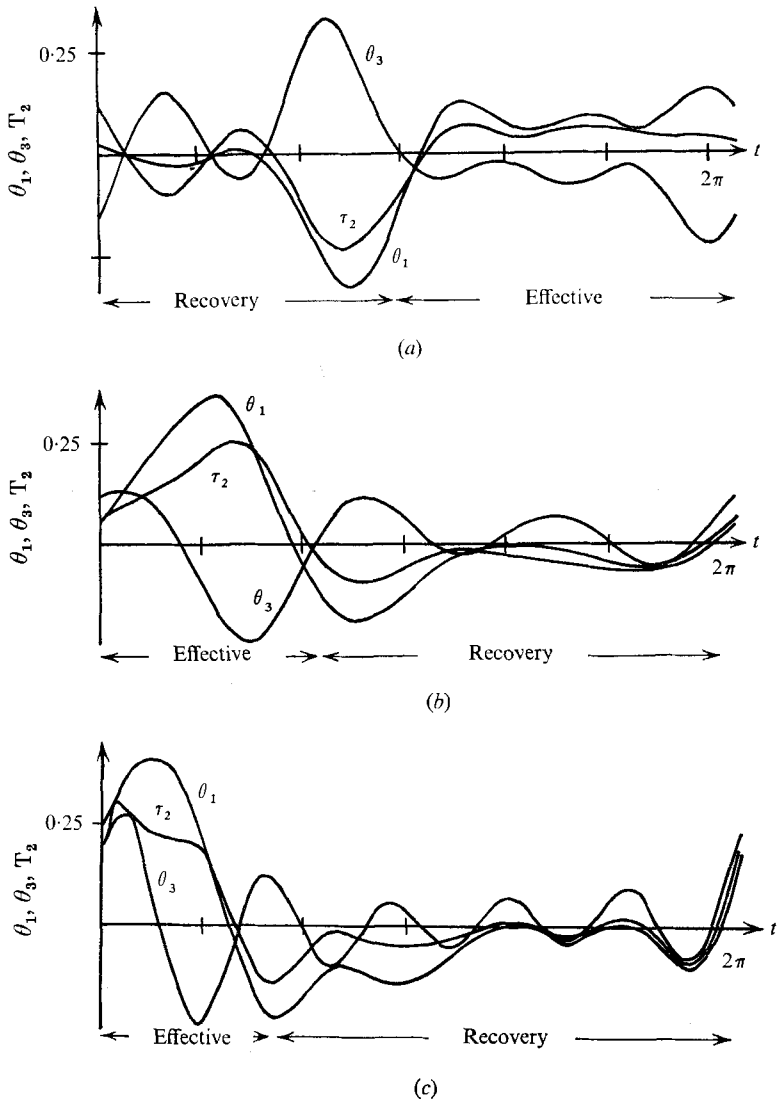

FIGURE 10. Graphs showing the forces and bending moments during one cycle of the beat for (*a*) *Opalina*, (*b*) *Paramecium* and (*c*) *Pleurobrachia*. The calculations are carried out for $\gamma = 1{\cdot}5$, $T = 150$ and $\kappa = \pm 0{\cdot}5$. Both the effective and recovery strokes are marked.

6.3. *Calculations of the force and bending moment*

The force and bending moment exerted by a cilium is of particular interest to the proto-zoologist as both experimental (Yoneda 1960, 1962) and theoretical work (Harris 1961) has been carried out on this subject. A review of this can be found in Holwill's (1966) paper. Harris (1961) calculated the bending moment by using Jeffery's (1923) formula for the couple produced by rotation of an ellipsoid in a viscous fluid. He obtains

$$M = 4\mu\sigma L^3/3 \log (L/r_0), \tag{38}$$

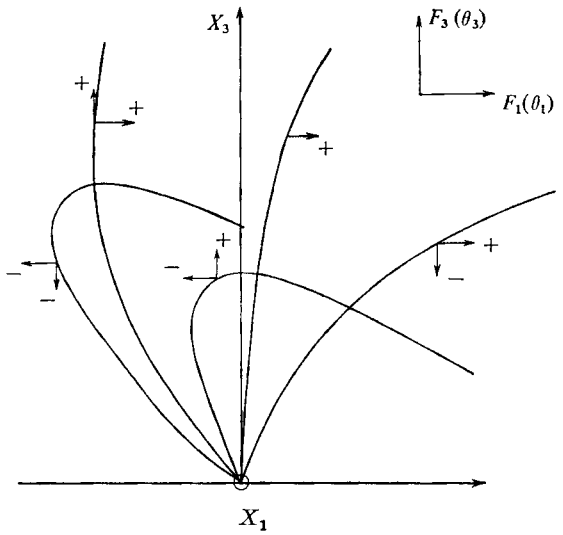

FIGURE 11. Diagram illustrating variations in sign of forces (F_1 and F_3) during beating cycle of a cilium.

where σ, L and r_0 are as defined in the previous analysis.

We define the force $\mathbf{F}$ and bending moment $\mathbf{M}$ about the base of a cilium by the following integrals:

$$\left.\begin{aligned} \mathbf{F} &= \frac{2\pi\sigma L^2\mu}{\log(L/r_0)+k_1}\boldsymbol{\theta}(t), \\ \mathbf{M} &= \frac{2\pi\sigma L^3\mu}{\log(L/r_0)+k_1}\boldsymbol{\tau}^*(t), \\ \text{where} \quad \boldsymbol{\theta}(t) &= \int_0^1 \left(\frac{\partial\hat{\boldsymbol{\xi}}}{\partial t} - \mathbf{U}(\xi_3) + V(\hat{\boldsymbol{\xi}})\right).\left(\gamma\mathbf{I} - (\gamma-1)\frac{\partial\hat{\boldsymbol{\xi}}}{\partial s}\frac{\partial\hat{\boldsymbol{\xi}}}{\partial s}\right) d\hat{s} \\ \text{and} \quad \boldsymbol{\tau}^*(t) &= \int_0^1 \hat{\boldsymbol{\xi}} \times \left(\gamma\mathbf{I} - (\gamma-1)\frac{\partial\hat{\boldsymbol{\xi}}}{\partial s}\frac{\partial\hat{\boldsymbol{\xi}}}{\partial s}\right).\left(\frac{\partial\hat{\boldsymbol{\xi}}}{\partial t} - \mathbf{U}(\xi_3) + \mathbf{V}(\hat{\boldsymbol{\xi}})\right) d\hat{s}. \end{aligned}\right\} \tag{39}$$

In the graphs of figure 10 we have plotted θ_1, θ_3 and τ_2^* against t, the time.

For the cases which exhibit antiplectic metachronism (i.e. *Paramecium* and *Pleurobrachia*) the force in the x_1 direction in the effective stroke is larger than that of the recovery stroke, although the force exerted over a cycle is very small and may be negative. This indicates, because inertial effects are neglected, that the drag on the surface of the organism is very small. One would intuitively expect little flow and low shear rates in this region of the cilia sublayer. In *Opalina*, which exhibits symplectic metachronism and which does not have the same distinction between the effective and recovery strokes, it is found that the force distribution is different. It appears that F_3 is large, relatively speaking, during the period when the bending wave is being propagated up the cilium immediately before its effective stroke (i.e. 3–5 in figure 6). To give us some understanding of the oscillation of sign experienced by F_3, figure 11 has been used to help explain this. During the effective stroke, F_3 changes sign as the cilium moves past the x_3 axis. It again changes sign during the propagation of

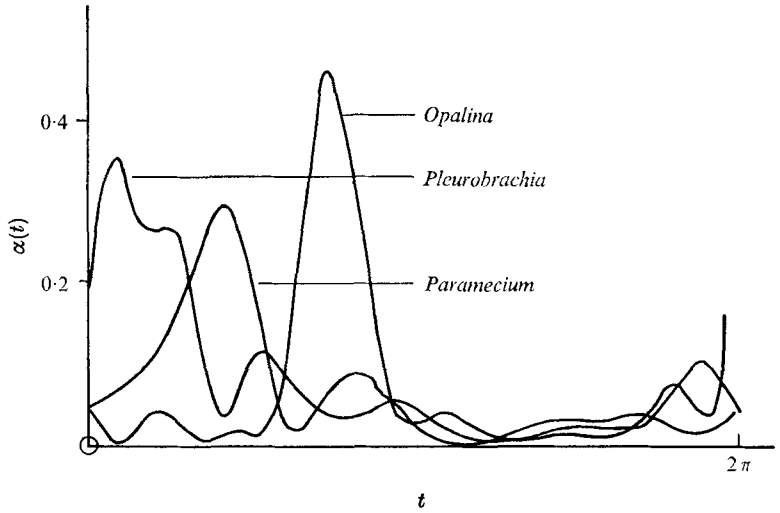

FIGURE 12. Graphs showing the rates of working for *Opalina*, *Paramecium* and *Pleurobrachia* with $\gamma = 1{\cdot}5$, T = 150 and $\kappa = \pm 0{\cdot}5$. The time spacing corresponds to those of figure 10.

the bending wave along the cilium, and may alter again before the beginning of the effective stroke. The bending moment follows a similar pattern to F_1 in that it is large and positive during the effective stroke and small and negative during the recovery stroke for antiplectic metachronism.

6.4. *Rate of working*

Another physical quantity which is of interest to both the zoologist and the fluid dynamicist is the rate of working P of a cilium. The rate of working P, as a function of time, can be defined as

$$\left.\begin{aligned} P &= \frac{2\pi\mu\sigma^2 L^3}{\log(L/r_0)+k_1}\,\alpha(t), \\ \alpha(t) &= \int_0^1 \hat{\mathbf{v}}\cdot\left(\gamma\mathbf{I}-(\gamma-1)\frac{\partial\hat{\boldsymbol{\xi}}}{\partial s}\frac{\partial\hat{\boldsymbol{\xi}}}{\partial s}\right)\cdot\hat{\mathbf{v}}\,d\hat{s}, \\ \text{with}\quad \hat{\mathbf{v}} &= \frac{\partial\hat{\boldsymbol{\xi}}}{\partial t}-\mathbf{U}(\hat{\boldsymbol{\xi}}_3)+\mathbf{V}(\hat{\boldsymbol{\xi}}). \end{aligned}\right\} \tag{40}$$

Graphs of $\alpha(t)$ are shown in figure 12. It is found in *Opalina* that the rate of working is largest during the period when the wave is being propagated up the cilium. For *Paramecium* and *Pleurobrachia* the rate of working is largest in the effective stroke. At the completion of the effective stroke there appears to be a short time when the cilium has a 'rest period'. The shape of the graphs is as expected because the forces and velocity are largest during the effective stroke in antiplectic metachronism while the same can be inferred for *Opalina* during the propagation of the bending wave. The energy dissipation over a complete cycle for the three organisms illustrated in figure 12 is approximately the same (i.e. $2\pi\bar{\alpha}$) in all cases. This indicates that for a given σ and L antiplectic metachronism appears to be the more efficient means of propulsion.

In conclusion, the calculations record many interesting and stimulating results which should encourage both more theoretical and experimental work on this subject. Backflow has yet to be observed experimentally, while improved calculations for the force, bending moments and energy dissipation will help the biophysicists with their understanding of the internal mechanisms of organelle movement.

The author acknowledges the support of a George Murray Scholarship from the University of Adelaide and a studentship from C.S.I.R.O. of Australia for this research. Comments and suggestions from Professor Sir James Lighthill are appreciated.

REFERENCES

BARTON, C. & RAYNOR, S. 1967 Analytic investigations of cilia induced mucous flow. *Bull. Math. Biophys.* **29**, 419–428.

BATCHELOR, G. K. 1970 Slender-body theory for particles of arbitrary cross-section in Stokes flow. *J. Fluid Mech.* **44**, 419–440.

BATCHELOR, G. K. 1971 The stress generated in a non-dilute suspension of elongated particles by pure straining motion. *J. Fluid Mech.* **46**, 813–829.

BLAKE, J. R. 1971*a* A spherical envelope approach to ciliary propulsion *J. Fluid Mech.* **46**, 199–208.

BLAKE, J. R. 1971*b* Infinite models for ciliary propulsion. *J. Fluid Mech.* **49**, 209–222.

BLAKE, J. R. 1971*c* A note on the image system for a Stokeslet in a no-slip boundary. *Proc. Camb. Phil. Soc.* **70**, 303–310.

BROKAW, C. J. 1970 Bending moments in free swimming flagella. *J. Exp. Biol.* **53**, 445–464.

CHWANG, A. T. & WU, T. Y. 1971 A note on the helical movements of micro-organisms. *Proc. Roy. Soc.* B **178**, 327–346.

COX, R. G. 1970 The motion of long slender bodies in a viscous fluid. Part 1. General theory. *J. Fluid Mech.* **44**, 791–810.

COX, R. G. 1971 The motion of long slender bodies in a viscous fluid. Part 2. Shear flow. *J. Fluid Mech.* **45**, 625–657.

GRAY, J. 1928 *Ciliary Movement.* Macmillan.

GRAY, J. & HANCOCK, G. J. 1955 The propulsion of sea-urchin spermatozoa. *J. Exp. Biol.* **32**, 808–814.

HANCOCK, G. J. 1953 The self propulsion of microscopic organisms through liquids. *Proc. Roy. Soc.* A **217**, 96–121.

HARRIS, J. E. 1961 In *The Cell and the Organism* (ed. J. A. Ramsay & V. B. Wigglesworth). Cambridge University Press.

HOLWILL, M. E. J. 1966 Physical aspects of flagellar movement. *Physiol. Rev.* **46**, 696–785.

HOLWILL, M. E. J. & SLEIGH, M. A. 1967*a* Film: Flagella and cilia. Department of Zoology, Bristol University.

HOLWILL, M. E. J. & SLEIGH, M. A. 1967*b* Propulsion by hispid flagella. *J. Exp. Biol.* **47**, 267–276.

JEFFERY, G. B. 1923 The motion of ellipsoidal particles immersed in a viscous fluid. *Proc. Roy. Soc.* A **102**, 161–179.

JONES, D. S. 1966 *Generalised Functions.* MacGraw-Hill.

KNIGHT-JONES, E. W. 1954 Relations between metachronism and the direction of ciliary beat in Metazoa. *Quart. J. Microsc. Sci.* **95**, 503–521.

LADYZHENSKAYA, O. A. 1963 *The Mathematical Theory of Viscous Incompressible Flow.* Gordon & Breach.

LAMB, H. 1932 *Hydrodynamics*. Cambridge University Press.

LIGHTHILL, M. J. 1958 *Fourier Analysis and Generalised Functions*. Cambridge University Press.

OSEEN, C. W. 1927 *Hydrodynamik*. Leipzig.

PRANDTL, L. 1952 *Essentials of Fluid Mechanics*. London: Blackie.

SHACK, W. J., FRAY, C. S. & LARDNER, T. J. 1971 Observations on the hydrodynamics and swimming motions of mammalian spermatozoa (preprint).

SLEIGH, M. A. 1962 *The Biology of Cilia and Flagella*. Pergamon.

SLEIGH, M. A. 1966 The coordination and control of cilia. *Symp. Soc. Exp. Biol.* **20**, 11–31.

SLEIGH, M. A. 1968 Patterns of ciliary beating. *Symp. Soc. Exp. Biol.* **22**, 131–150.

SLEIGH, M. A. & AIELLO, E. 1971 The movement of water by cilia (preprint).

TAYLOR, G. I. 1951 Analysis of the swimming of microscopic organisms. *Proc. Roy. Soc.* A **209**, 447–461.

TILLETT, J. P. K. 1970 Axial and transverse Stokes flow past slender axisymmetric bodies. *J. Fluid Mech.* **44**, 401–418.

TUCK, E. O. 1968 Toward the calculation and minimization of Stokes drag on bodies of arbitrary shape. *Trans. Inst. Engrs. Aust.* **3**, 29–32.

WINET, H. 1970 Film: Flow fields over swimming ciliated cells. Californian Institute of Technology.

YONEDA, M. 1960 Force exerted by a single cilium of *Mytilus edulis*. I. *J. exp. Biol.* **37**, 461–468.

YONEDA, M. 1962 Force exerted by a single cilium in *Mytilus*. II. *J. exp. Biol.* **39**, 307–317.